HaP / LP-SBA-15 Nanocomposite for efficient removal of fluoride from contaminated water

Claudia G. Lopez*, Jorgelina Cussa and Oscar A. Anunziata

Centro de Investigación en Nanociencia y Nanotecnología (NANOTEC), Facultad Regional Córdoba, Universidad Tecnológica Nacional, Maestro López y Cruz Roja Argentina, 5016, Córdoba, Argentina.

Abstract

Hydroxyapatite (HaP) composites and highly ordered large pore mesoporous silica, such as LP-SBA-15 (Large Pore-SBA-15), were developed, characterized by XRD, BET, FTIR and HRTEM, and applied properly to fluoride removal from contaminated water. The proposed procedure to prepare HaP/LP-SBA-15 was successful, which acts as supports to anchor the HaP crystals, in nanometer-scale (<12 nm), with higher fluoride retention from contaminated water. The free OH- groups of HaP nanocrystals, inside the host, permitted fluoride retention with high capacity. The fluoride holding activity was over 3 orders of magnitude higher than pure HaP.

HaP / LP-SBA-15 Nanocomposite for efficient removal of fluoride from contaminated water

Claudia G. Lopez*, Jorgelina Cussa and Oscar A. Anunziata

Centro de Investigación en Nanociencia y Nanotecnología (NANOTEC), Facultad Regional Córdoba, Universidad Tecnológica Nacional, Maestro López y Cruz Roja Argentina, 5016, Córdoba, Argentina.

Abstract

Hydroxyapatite (HaP) composites and highly ordered large pore mesoporous silica, such as LP-SBA-15 (Large Pore-SBA-15), were developed, characterized by XRD, BET, FTIR, and HRTEM, applied to fluoride removal from contaminated water. The proposed procedure to prepare HaP/LP-SBA-15 was successful, which acts as supports to anchor the HaP crystals, in nanometer-scale (<12 nm), with higher fluoride retention from contaminated water. The free OH- groups of HaP nanocrystals, inside the host, permitted fluoride retention with high capacity. The fluoride holding activity was over 3 orders of magnitude higher than pure HaP.

Keywords: F$^-$ retention; water; HaP/ LP-SBA-15; nanocomposites

1. Introduction

Numerous approaches, such as precipitation-coagulation [1], membrane technology membranes [2,3], ion exchange [4], and adsorption [5, 6]. in the past decades to decrease fluoride in water and reach the security level of drinking water. Among all the above methods, fluoride adsorption on adsorbents is increasingly receiving attention due to its advantages of easy design and operation, and low cost [7]. Different types of adsorbents, such as metallic adsorbents [8-10], carbon adsorbents [11, 12], carbon materials [12,13], natural materials [13], and biosorbents [14-16]. have been used to remove fluoride from water. Recently, zirconium-based materials have proven to be good candidates for the removal of fluoride from water, due to the high affinity of the tetravalent metal ions Zr (IV) to the highly electronegative fluoride ion. Also, zirconium-based materials have good thermal and chemical stability. Metal-organic frameworks (MOFs) are multifunctional porous materials with potential in various areas [17].with potential in various areas [17]. Recently, MOFs have also been as new adsorbents for fluoride adsorption because of their surface functional groups and ordered atomic arrangement [18]. Calcium phosphate apatites are compounds of the formula $Ca_5(PO_4)_3X$, where X can be an F$^-$ (fluorapatite, FaP), OH$^-$ (hydroxyapatite, HaP), or a Cl$^-$ ion (chlorapatite). One ion is replaced by another of the same sign but of a different charge. Neutrality is maintained by substitutions of ions with dissimilar charges or vacancies elsewhere [19]. Dalas, et.al [20] studied the crystallization of HaP (hydroxiapatite) on polymers containing - C-N groups, from supersaturated solutions of HaP. This method was particularly useful to study the formation of new phases on the substrates in which HaP was deposited. The growth of hydroxyapatite on silica gels in the presence of organic additives was

studied by Rivera-Muñoz et al. [21]. Laghzizil et al. [22] have been correlated the results of fluorization of HaP with the Physico-chemical properties of the same ones. Recently, we published the activity of HaP/ MCM-41 and HaP-SBA-15 composites, for fluoride retention [23]. We developed a technique of preparation of nanocrystalline HaP (ex-situ), and via by the same procedure, but in the presence of the respective hosts, forming in situ composites. We compared the capacity of F^- retention from contaminated water, respect to a commercial one. Recently, we report our first results of the development of LP-SBA.15 [24]. In the present work, we correlated fluoride retention from contaminated water, with the physicochemical properties of HaP/LP-SBA-15 nanocomposites.

2. Experimental

Hosts synthesis: Conventional mesostructured SBA-15 silica, presenting hexagonally-arranged unidirectional pores with mean pore sizes in the range of 6 - 9 nm [25].

Specifically, 2.4 g of the template ingredient (Pluronic 123 copolymer, Aldrich) and 0.027 g of NH4F dissolved in 85 mL HCl (1.3 M) at ambient temperature were placed in a water bath at 17ºC for 1h. Later, 5.5 mL of tetraethylortosilicate (TEOS, Aldrich) and 1.2 mL of 1,3,5-triisopropyl benzene (TIPB, Aldrich) were incorporated. Later, 5.5 mL of tetraethylortosilicate (TEOS, Aldrich) and 1.2 mL of 1,3,5-triisopropyl benzene (TIPB, Aldrich) were incorporated and maintained with mechanical agitation at this temperature for 24h. The remaining white suspensions were then aged at 100°C (LP) under static and autogenic pressure for 24 h. The solid products were collected by filtration. To eliminate the template agent, the solid obtained was heated under a flow of N2 at 20 mL/min at 470 °C and then heated again at 550 °C under static air for 6 h. The resultant mesoporous material large pore SBA-15 was named LP-SBA-15. To prepare HaP/host (HaP-in-situ) was followed the same procedure described by us [23], in presence of LP-SBA-15 added at the first 0.5h, of the reaction time that was employed to prepare HaP ex-situ. The suspensions were vigorously stirred for 4 h, at 60ºC, filtered, washed with triple-distilled carbon dioxide-free water, and then dried at 100ºC for 4 h. The composite was activated by heating at 550ºC in N_2 flow for 5 h, then calcined up to 500ºC at a heating rate of 5ºC/min from 100ºC for 4h. Commercial hydroxyapatite (CHaP), also was used in this study, provided by Bio-gel HTP, marketed by BIO-RAD®.

3. Fluoride retention essay

Fluoride ion solutions were prepared using a Teflon device with magnetic stirring, specially designed to bubble N_2 to avoid CO_2 contamination at 25ºC. The pH of the solutions was measured with a Mettler pH meter with combined glass electrodes; the instrument was calibrated with buffers of pH = 4 and 7.5. Ion F^- concentration was determined using a specific electrode for F^-, dynamic range between 1 to 300 ppm. Besides, F^- traces were followed by FTIR. Experimental conditions: 1.8 g of HaP in 100 mL of NaF solution with the initial concentration of 9 x10^{-2} M. The weight of the materials employed was normalized on HaP base.

4. Characterization

BET studies were performed with an ASAP 2010 Micromeritics apparatus. Diffraction patterns were performed with a Philips X'Pert PRO PANalytical diffractometer under Cu Kα radiation. A JASCO

5300 spectrometer was employed to obtain the FTIR characterization. For the absorption region of the host lattice, 0.05wt% wafers were prepared in KBr. High-resolution transmission electron microscopy (HRTEM) images of some representative samples were acquired using a JEOL-200 CX electron microscope.

5. Results and discussion

XRD and BET

The surface area of the HaP commercial sample (CHaP), measured by the single-point BET (N_2) method, and was 69 m^2/g. The surface areas were 960 for LP-SBA-15 (pore volume 1 mL/g) and 390 m^2/g for Hap/LP-SBA-15 respectively. The pore diameter of the hosts was: 12 nm for LP-SBA-15. The composite HaP/LP-SBA-15 isotherms show a residual pore volume of 0.80-0.83 mL per gram for LP-SBA-15.

The low angle XRD pattern (Fig. 1) for the host LP-SBA-15 displays a high reflection peak (1 0 0) and two minor peaks (second-and third-order peaks), corresponding to the diffraction planes (1 1 0) and (2 0 0)). These peaks can be indexed with a hexagonal crystallographic structure of the P6mm group. The pattern diffraction peaks confirm a high crystallinity or long-range order structure in nanostructured host. The XRD pattern of, pure HaP prepared ex-situ by us, HaP/LP-SBA-15 composites are illustrated in Fig. 2.
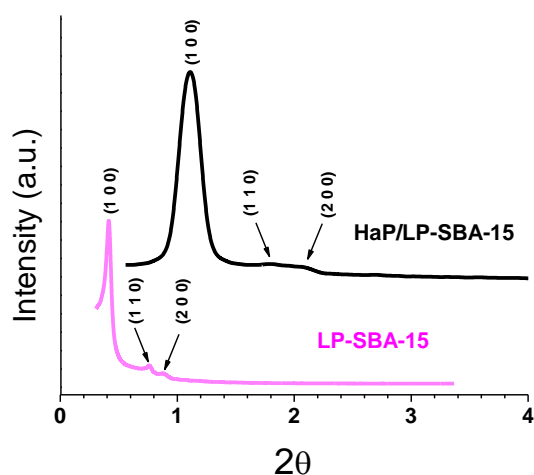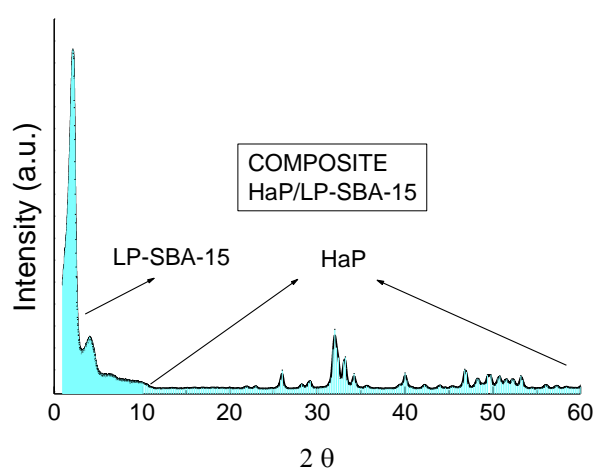
Figure 1: XRD of LP-SBA-15   **Figure 2:** XRD of HaP/LP-SBA-15

FTIR studies

FTIR data of HaP/LP-SBA-15 with the assigned bands (previous to its use for the determination of retention of F$^-$) are shown in figure 3. The P–O stretching IR mode appears at ~ 970 cm^{-1} in the spectra of the HaP. The PO_4 region appears as a very strong band at ~1030 cm^{-1}, whereas the band at 3570 cm^{-1} is assigned to the OH stretching mode [19]. The well-defined bands at 650 and 564 cm^{-1} are attributed to the components of asymmetrical deformation O-P-O. HaP/LP-SBA-15 composites, with HaP crystals (in the nm range), generate difficulty for the band identification. FTIR of HaP/LP-SBA-15 (fig. 3) also shows bands corresponding to LP-SBA-15, at 1080, 1227 and 1669 cm^{-1} (T–O asymmetric

stretching, internal and external respectively), 800 cm^{-1} (T–O symmetric stretching) are due to TO$_4$ vibrations (T = Si). By FTIR of the composite in the OH stretching zone, one strong signal at 3570 cm^{-1} due to OH$^-$ of HaP is observed [19]. This band must remain intact so that the capacity of F$^-$ retention of composite is not altered for a longer time as possible, (fig. 3).
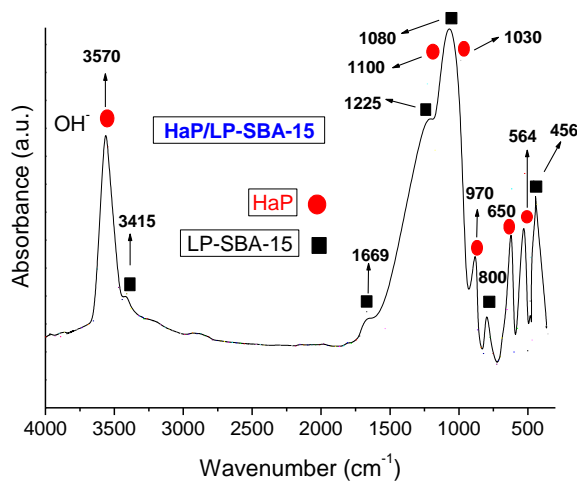

Figure 3: FTIR of HaP/LP-SBA-15 nanocomposite.

^{27}Al NMR-MAS results of LP-SBA-15 samples showed one intense peak at 53 ppm in the samples, assigned to Al$^{IV}_{Td}$ form, although a very low signal at 0 ppm due to octahedral extra framework aluminum (Al$^{IV}_{Oc}$) for LP--SBA-15b materials.

HRTEM

The HRTEM images illustrated in Fig. 4, reveals the existence of a long-range hexagonal arrangement of nanosized mesopores. The higher-order reflections are still discernable clearly in the sample HaP/LP-SBA-15 compared with the HRTEM of the hosts reported in the literature. Thus the nanosized crystals of HaP are within the mesostructure of the hosts. The size and shape (SEM, not showed) of the hosts indicated, a good morphology of the crystals, without other phases, and typical of the materials. SBA-15 images reveal that it consists of many rope-like domains with relatively uniform sizes of 1.5-2.5 µm, which are aggregated into wheat-like macrostructures.
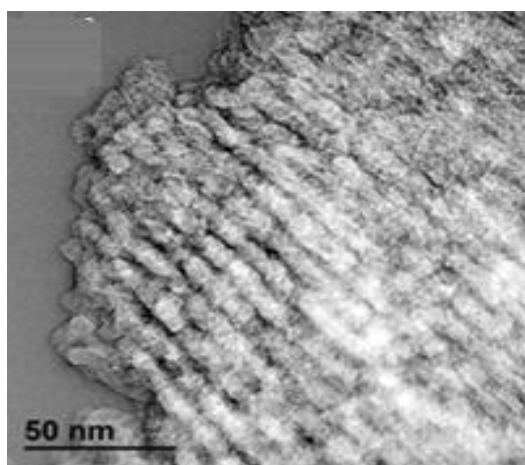

Figure 4: HRTEM of HaP/-LP-SBA-15

Fluoride Retention

Figure 6 shows the F⁻ retention capacity of the HaP/LP-SBA-15 composite, and HaP commercial sample (CHap). The method used for the host inclusion (not found in literature) seems to be adequate since the OH⁻ groups of HaP were not blocked. In the case of HaP (ex-situ), its lower crystal size favored the F⁻ retention compared with the commercial one.

LP-SBA-15 acts as supports to anchor the HaP crystals, in nanometer-scale (<12 nm), with higher fluoride retention from contaminated water. In fig 6, we can see that the fluoride retention by the hosts is not significant. Fluoride is not retained in the solution, but by the composite. The results demonstrated first, fast retention of fluoride from 0 to 6 hours and, soon decay slowly until reaching the stationary state, about 15 hours. The final concentration of fluoride ion was: 0.2 x10⁻² M, for HaP/LP-SBA-15.

The results suggest are that the OH⁻ remains intact due to fluorination due to a high dispersion with the lower size of HaP nanocrystals and higher OH⁻ site per gram of the active material.
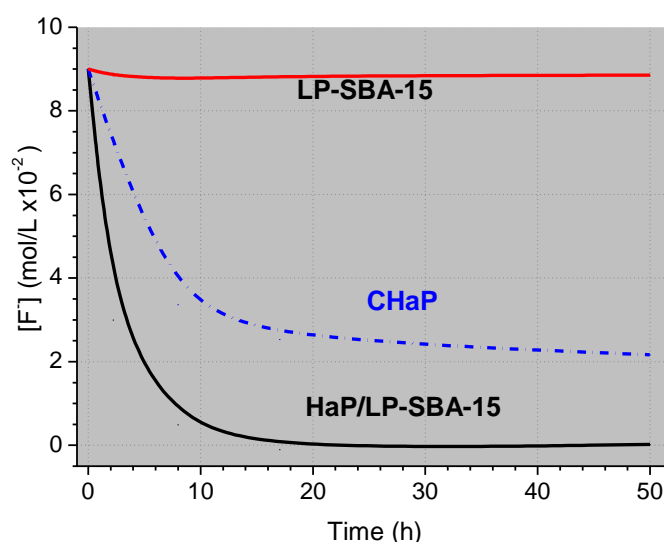

Figure 6: Capacity of F⁻ retention from contaminated water of the samples against the time.

6. Conclusions

LP-SBA-15 materials have good structural and textural properties, useful to acts as hosts incorporating nanocrystals of hydroxyapatite, forming active composites. By HRTEM. FTIR, XRD, we found that the HaP nanocrystals are within the hosts, and not on the external surface, indicated good incorporation of nano-crystals in the host with sizes of pores higher than 12 nm. Is noticeable the increasing of the fluoride retention with the surface area, and diameter pore, anchoring nanocrystals of HaP, leaving free de OH⁻ groups of the HaP. The capacity of fluoride retention of the HaP/hosts increases more than three orders of magnitude concerning pure HaP.

7. Acknowledgment

8. References

[1] W.X. Gong, J.H. Qu, R.P. Liu, H.C. Lan, Colloid Surf. A 395 (2012) 88–93.
[2] A. Tor, J. Hazard. Mater 141 (2007) 814–818.
[3] J.Y. He, K. Chen, X.G. Cai, Y.L. Li, C.M. Wang, K.S. Zhang, Z. Jin, F.L. Meng,
X.G. Wang, L.T. Kong, J.H. Liu, J. Colloid Interface Sci. 490 (2017) 97–107.
[4] N. Viswanathan, S. Meenakshi, J. Hazard. Mater 162 (2009) 920–930.
[5] X.P. Liao, B. Shi, Environ. Sci. Technol. 39 (2005) 4628–4632.
[6] L.H. Velazquez-Jimenez, R.H. Hurt, J. Matos, J.R. Rangel-Mendez, Environ. Sci.
Technol. 48 (2014) 1166–1174.
[7] A. Bhatnagar, E. Kumar, M. Sillanpää, Chem. Eng. J. 171 (2011) 811–840.
[8] B. Zhao, Y. Zhang, X.M. Dou, X.M. Wu, M. Yang, Chem. Eng. J. 185–186 (2012)
211–218.
[9] C.Y. Jing, J.L. Cui, Y.Y. Huang, A. Li, ACS Appl. Mater. Interfaces 4 (2012) 714–720.
[10] Z. Jin, Y. Jia, K.S. Zhang, L.T. Kong, B. Sun, W. Shen, F.L. Meng, J.H. Liu, J. Alloy.
Compd. 675 (2016) 292–300.
[11] E. Vences-Alvarez, L.H. Velazquez-Jimenez, L.F. Chazaro-Ruiz, P.E. Diaz-Flores,
J.R. Rangel-Mendez, J. Colloid Interface Sci. 455 (2015) 194–202.
[12] M.H. Dehghani, G.A. Haghighat, K. Yetilmezsoy, G. Mckay, B. Heibati, I. Tyagi,
S. Agarwal, V.K. Gupta, J. Mol. Liq. 216 (2016) 401–410.
[13] Y. Çengeloğlu, E. Kır, M. Ersöz, Sep. Purif. Technol. 28 (2002) 81–86.
[14] H.M. Cai, L.Y. Xu, G.J. Chen, C.Y. Peng, F. Ke, Z.Q. Liu, D.X. Li, Z.Z. Zhang,
X.C. Wan, Appl. Surf. Sci. 375 (2016) 74–84.
[15] L.Y. Xu, G.J. Chen, C.Y. Peng, H.H. Qiao, F. Ke, R.Y. Hou, D.X. Li, H.M. Cai,
X.C. Wan, Carbohyd. Polym. 160 (2017) 82–89.
[16] H. Paudyal, B. Pangeni, K.N. Ghimire, K. Inoue, K. Ohto, H. Kawakita, S. Alam,
Chem. Eng. J. 195–196 (2012) 289–296.
[17] Z.Y. Gu, C.X. Yang, N. Chang, X.P. Yan, Acc. Chem. Res. 45 (2012) 734–745.
[18] P. Kumar, A. Pournara, K.H. Kim, V. Bansal, S. Rapti, M.J. Manos, Prog. Mater. Sci.
86 (2017) 25–74.
[19] J. Elliot (1994) Structure and chemistry of the apatite and other calcium orthophosphates. Elsevier,
Amsterdam, and references therein.
[20] E. Dalas, A. Chrissanthopoulos (2003) J. of Cryst. Growth. 255: 163.
[21] E. Rivera-Muñoz, W. Brostow, R. Rodríguez, V. Castaño (2001) Mat. Res. Innovat. 42: 22-30.
[22] A. Laghzizil, N. Elhrech, O. Britel, A. Bouhaouss (2000) J. of Fluoride Chem. 10:169-176.
[23] O. Anunziata, A. Beltramone, J. Cussa (2007) In: Stud. Surf. Scie. and Catal., Recent Progress in
Mesostructured Materials, Elsevier, Amsterdam.
[24] J. Cussa, A. Prados, J. Juarez, A. Beltramone, O. Anunziata (2019) 19th International Zeolite
Conference (IZC-19)
[25] J. Juárez, M. Gómez Costa, O. Anunziata (2015) Int. J. Energy Res. 39, 128–139.